Supplementary Material:

Improvement of Piglet Rearing's Energy Efficiency and Sustainability using Air-to-Air Heat Exchangers – A two-year case study

Hauke F. Deeken, Alexandra Lengling, Manuel S. Krommweh, Wolfgang Büscher

S1. Nomenclature

Parameter	Unit	Meaning
A	-	Exhaust air purification system
ABS-HH	-	High heat acrylonitrile butadiene styrene
AP	-	Animal Place
C_{el}	EUR kWh_{el}^{-1}	Energy costs for electrical energy (e.g., electricity of the German power grid)
C_{th}	EUR kWh_{th}^{-1}	Energy costs for thermal energy (e.g., combustion of LNG)
Case 1	-	Planning Case 1: Piglet rearing barn building with heat recovery, reality
Case 2	-	Planning Case 2: Piglet rearing barn building without heat recovery, hypothetical case
CIGR		International Commission of Agricultural Engineering
CO_2	-	Carbon Dioxide
CO_{2eq}	-	Carbon Dioxide equivalents
CO_2 $Emissions_A$	kg CO_2	CO_2 emissions based on the electrical energy consumption of the exhaust air purification system (A)
$COP_{heating}$	-	Coefficient of Performance during heating of the heat recovery
$COP_{HR,heating}$	-	Coefficient of Performance, the relation of electrical power input consumption to operate a heat recovery system (two heat exchangers) in the barn building's ventilation system divided by the thermal power of the heat recovery system
$COP_{V,heating}$	-	Coefficient of Performance, the relation of electrical power input to operate the ventilation system divided by the thermal power of the heat recovery system
$COP_{VA,heating}$	-	Coefficient of Performance, the relation of electrical power input to operate the ventilation system and the exhaust air purification system divided by the thermal power of the heat recovery system
c_{pl}	Wh_{th} $(kg\ K)^{-1}$	Specific heat capacity of dry air c_{pl} = 1.005 kJ_{th} $(kg\ K)^{-1}$ = 0.28 Wh_{th} $(kg\ K)^{-1}$
ε	-	Effectiveness of the heat recovery system (heat exchangers)
el	-	electrical
Energy $costs_V$	EUR	Energy costs based on the electrical energy consumption of the ventilation system (V)
GER	-	Germany
GHG	-	Greenhouse gases
HR		Heat recovery
HVAC		Heating, Ventilation, and Air Conditioning
L x W x H	-	Length x Width x Height

Parameter	Unit	Meaning
LNG	-	Liquefied Natural Gas
LU	-	Livestock unit: 1 LU = 500 kg animal life weight
$\dot{m}$	kg h^{-1}	Air mass flow rate
$\dot{m}_1$	kg h^{-1}	Exhaust air mass flow rate
$\dot{m}_2$	kg h^{-1}	Supply air mass flow rate
$\dot{m}_{min}$	kg h^{-1}	Minimum of exhaust air mass flow rate or supply air mass flow rate
$m_{CO2,el}$	(kg CO_2) kWh_{el}^{-1}	CO_2 emission factor for electrical energy (e.g., electricity of the German power grid)
$m_{CO2,th}$	(kg CO_2) kWh_{th}^{-1}	CO_2 emission factor for thermal energy (e.g., combustion of LNG)
NH_3	-	Ammonia
P_{el}	kW_{el}	Electrical power input of specific consumers
$PF_{heating}$		Performance factor, based on the $COP_{heating}$
$PF_{HR,heating}$		Performance factor, the relation of electrical energy consumption to operate a heat recovery system (two heat exchangers) in the barn building's ventilation system divided by the thermal energy recovered using the heat recovery system, based on the $COP_{HR,heating}$
$PF_{V,heating}$		Performance factor, the relation of electrical energy consumption to operate the ventilation system divided by the thermal energy recovered using the heat recovery system, based on the $COP_{V,heating}$
$PF_{VA,heating}$		Performance factor, the relation of electrical energy consumption to operate the ventilation system and the exhaust air purification system divided by the thermal energy recovered using the heat recovery system, based on the $COP_{VA,heating}$
$\dot{Q}_{HR,th}$	kW_{th}	Thermal power of the heat recovery system
$\dot{Q}_{max,th}$	kW_{th}	Maximum possible thermal power potential of the heat recovery system
$Q_{A,el}$	kWh_{el}	Electrical energy consumption of the exhaust air purification system (A)
Q_{Case1}	$kWh_{el,th}$	Energy consumption to operate the barn building in Case 1 (with heat recovery)
Q_{Case2}	$kWh_{el,th}$	Energy consumption to operate the barn building in Case 2 (without heat recovery)
$Q_{extra\ LNG,Case2,th}$	kWh_{th}	$= Q_{HR,th}$ = Additional thermal energy provided due to the needed combustion of LNG in Case 2 corresponds to the recovered thermal energy in Case 1
$Q_{HR,el}$	kWh_{el}	Electrical energy consumption to operate a heat recovery system (two heat exchangers) in the barn building's ventilation system
$Q_{HR,th}$	kWh_{th}	Thermal energy recovered by the heat recovery system (two heat exchangers)
$Q_{LNG,Case1,th}$	kWh_{th}	Thermal energy provided due to combustion of LNG in Case 1
Q_{total}	$kWh_{el,th}$	Energy consumption to operate the barn building
$Q_{total,el}$	kWh_{el}	Electrical energy consumption to operate the barn building
$Q_{total,th}$	kWh_{th}	Thermal energy consumption to operate the barn building

Parameter	Unit	Meaning
$Q_{V,Case\ 1,el}$	kWh_{el}	Electrical energy consumption of the ventilation system (V) in Case 1 (with heat recovery system)
$Q_{V,Case\ 2,el}$	kWh_{el}	Electrical energy consumption of the ventilation system (V) in Case 2 (without heat recovery system)
t_0	°C	Outside air temperature
$t_{0,max}$	°C	Maximum daily outside air temperature
$t_{0,min}$	°C	Minimum daily outside air temperature
t_{11}	°C	Exhaust air temperature
t_{12}	°C	Outlet air temperature
t_{21}	°C	Fresh air temperature
t_{22}	°C	Supply air temperature
$t_{22,max}$	°C	Maximum daily supply air temperature
$t_{22,min}$	°C	Minimum daily supply air temperature
th	-	thermal
USA	-	United States of America
V	-	Ventilation system
$\dot{V}$	$m^3\ h^{-1}$	Air volume flow rate
Year 1	-	First trial year: 17. December 2019 – 15. December 2020
Year 2	-	Second trial year: 16. December 2020 – 15. December 2021

S2. Heat Exchanger & Sensors

Table S1. Technical specifications and parameters of each air-to-air-heat exchanger used in the presented trial.

Parameter	Specification
Manufacturer	hdt Anlagenbau GmbH, Diepholz, Germany
Product Type	WT-BTK 200
Heat recovery principle	Recuperative air-to-air heat exchanger (turbulent counter-flow)
Outside dimensions	332 × 114.6 × 442 cm (L × W × H)
Outer shell material	Insulating composite panels (expanded polystyrene, EPS) with a stable fiberglass/polyester coating and roving mat fiberglass/polyester profiles
Outer shell thickness	≈ 25.3 mm
Outer shell thermal conductivity	≈ 0.035 W_{th} (m K)$^{-1}$
Heat exchanger modules (=pair of plates)	46
Heat exchanger surface	≈ 266.64 m^2
Specific heat exchanger surface	≈ 0.01587 m^2 m^{-3} h^{-1} (at nominal max. air flow rate 16,800 m^3 h^{-1})
Heat exchanger plates material	High heat acrylonitrile butadiene styrene (ABS-HH): $(C_8H_8)_x$ $(C_4H_6)_y$ $(C_3H_3N)_z$
Heat exchanger plates structure	Thermoformed helical surface
Heat exchanger plates thickness	0.5 mm
Heat exchanger plates thermal conductivity	≈ 0.180 – 0.250 W_{th} (K m)$^{-1}$
Heat exchanger plates' nominal thermal transmittance (U-value)	≈ 5.79 W_{th} (K m^2)$^{-1}$

Table S2. Technical specifications and parameters of the temperature sensors used in the presented trial.

Sensor	Parameter	Specification
Testo 174 T	Manufacturer	Testo SE & Co. KGaA, Titisee-Neustadt, Germany
	Sensor Type	NTC (Negative Temperature Coefficient) Thermistor
	Measuring Interval	15 min
	Measuring Range Temperature	-30 – +70°C
	Measuring Accuracy Temperature	±0.5°C
	Measuring Points	1× t_0, 1× t_{11}, 2× t_{12}, 1× t_{21}, 1× t_{22}
TGP-4500	Manufacturer	Gemini Data Loggers Ltd, Chichester, United Kingdom
	Sensor Type	10K NTC (Negative Temperature Coefficient) Thermistor (internal probe)
	Measuring Interval	15 min
	Measuring Range Temperature	-25 – +85°C
	Measuring Accuracy Temperature	±0.4 – 0.9°C
	Measuring Range Relative Humidity	0 – 100%
	Measuring Accuracy Relative Humidity	±3.0% at 25°C
	Measuring Points	1× t_{11}, 1× t_{21}
TGP-4505	Manufacturer	Gemini Data Loggers Ltd, Chichester, United Kingdom
	Sensor Type	10K NTC (Negative Temperature Coefficient) Thermistor (external probe)
	Measuring Interval	15 min
	Measuring Range Temperature	-25 – +85°C
	Measuring Accuracy Temperature	±0.35 – 0.50°C
	Measuring Range Relative Humidity	0 – 100%
	Measuring Accuracy Relative Humidity	±3.0% at 25°C
	Measuring Points	1× t_0, 1× t_{11}, 1× t_{21}, 1× t_{22}
WTR 190-A1-1A2/PT1000	Manufacturer	promesstec GmbH, Schüttorf, Germany
	Sensor Type	PT-1000 (Resistance Temperature Detector, RTD)
	Measuring Interval	15 min
	Measuring Range Temperature	-50 – +130°C
	Measuring Accuracy Temperature	± (0.15 + 0.002 × t)°C Example for t = 20°C: ± (0.15 + 0.002 × 20)°C = 0.19°C
	Measuring Points	1× t_0, 1× t_{11}, 1× t_{12}, 1× t_{21}, 1× t_{22}

S3. Characteristics of the fans and calculation of the air flow rates for the example of the exhaust air fans (A3G990-AZ02-35, ebm-papst Mulfingen GmbH & Co. KG, Mulfingen, Germany)

The calculation of the air volume flow rates took place in several steps (the similar procedure applied for the supply air fans, Ziehl-Abegg SE, Künzelsau, Germany; not shown for reasons of space):

1. Preliminary tests were conducted to investigate the performance of the fans in the barn building. For this purpose, the ventilation system was controlled manually for short periods of time so that the entire power spectrum of the system and the fans was controlled. During this test, the following dependencies were tested:
    a. Which analog control of the fans is present at each 15-minute interval? These values were derived up to 6th August 2020 from the percentage of the performance of the entire ventilation system [%] and later output directly by the system control software.
    b. What is the dependence of the operating parameters of the fans on their control [V]? For this purpose, the speed [n min^{-1}] and the electrical power input [W] were recorded as a function of the analog control (see Figure S1). In detail, the correlations show an increasing divergence with increasing analog control (> 6.5 V; see Section S4).

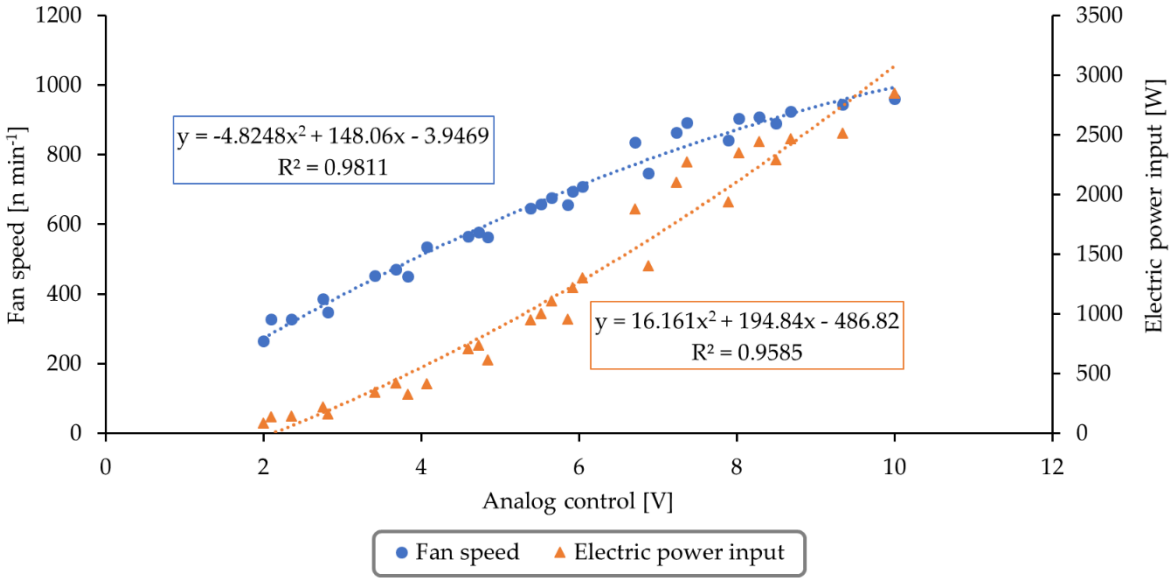

Figure S1. Fan Speed [n min^{-1}] and Electric Power Input [W] of ebm exhaust air fans in the investigated barn building depending on the analog control [V] of the fans.

2. Differential pressure sensors were installed within the ventilation system of the barn building, which measured the differential pressures (measuring point vs. atmospheric pressure). The following measuring points apply I) the central exhaust air collection duct, II) the heat exchanger (right in front of the corresponding exhaust/outgoing air fan), and III) the pressure chamber beneath the synthetic fillers of the bio-scrubber. An additional differential pressure sensor was installed IV) in the supply air duct, measuring the pressure difference in front vs. behind the supply air fan. From these differential pressures, the pressure differences between various points in

the ventilation system (e.g., in front of versus behind the fans) were calculated. Following pressure differences apply for the various fans, which were used for further calculations:

a. Supply air fans:
   supply air duct in front of the fan
   VS.
   supply air duct behind the fan
b. Exhaust air fans heat exchangers (Case 1, bypass air shutters open or closed):
   heat exchanger, right in front of the corresponding exhaust/outgoing air fan
   VS.
   pressure chamber beneath the synthetic fillers of the bio-scrubber
c. Exhaust air fans bypass groups 1 and 2:
   central exhaust air collection duct
   VS.
   pressure chamber beneath the synthetic fillers of the bio-scrubber

3. The information provided by the fan manufacturers regarding the performance parameters of the fan models in the calibration and test bench measurements was used to calculate the air volume flow rates conveyed.
   For this purpose, the information in the calibration and measurement protocols was used on the one hand, as well as detailed information in 'ebm's planning and control software (ebm-papst FanScout).
   Data tables were created from these test bench measurements, which included the fan speed, the pressure differences (in front of vs. behind the fan as measured in the barn building, see 2.), and the airflow rates conveyed.
   For further calculation, these data were grouped for the pressure differences. For each integer pressure difference, a regression line was derived, indicating the airflow rate of the fan as a function of the fan speed (see Figure S3).

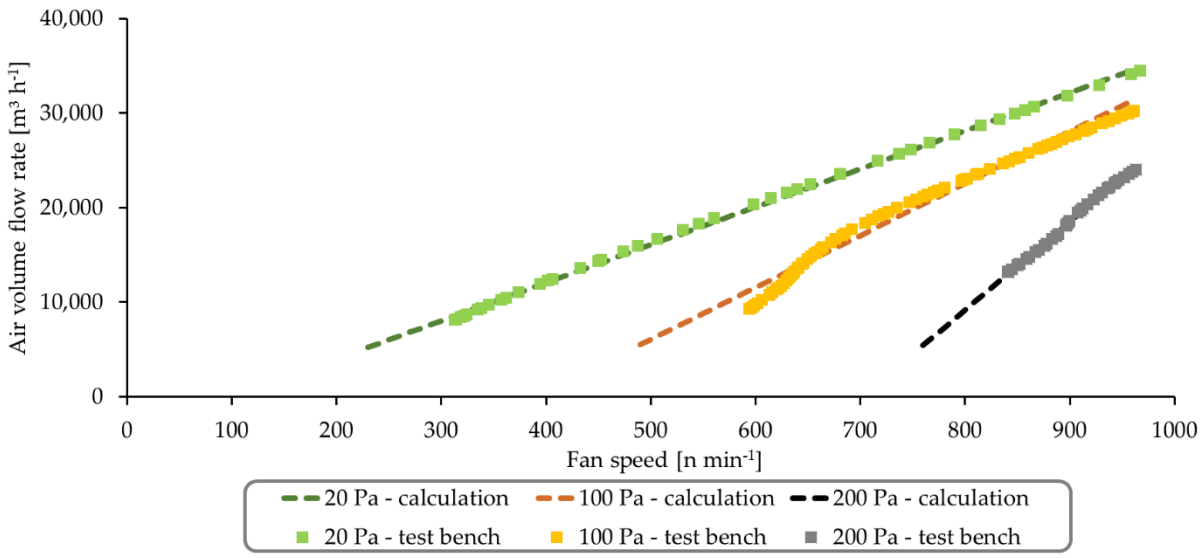

Figure S2. Air volume flow rate [m^3 h^{-1}] of the ebm exhaust air fans depending on the fan speed [n min^{-1}] for exemplary pressure differences [Pa].

4. The measured data of the differential pressure sensors in the barn building [Pa], as well as the fan control [V], and the resulting fan speed [n min^{-1}], were available for each 15-minute measurement interval. For each measurement interval, the linear regression line was used to calculate the air volume flow rate [m^3 h^{-1}] as a function of the speed at a given pressure difference. This air volume flow was converted into an air mass flow rate ($\dot{m}$ [m^3 h^{-1}] $= \dot{V} * (-0.00482 * t_{22} + 1.274)$; see Section 2.4).

These calculation steps were applied for all fans in the barn building (6× exhaust air fans using ebm-papst fans, 2× supply air fans using Ziehl-Abbegg fans).

The calculated air flow rates were subsequently used to calculate the performance parameters of the heat recovery system (two heat exchangers), including thermal power [W].

S4. Uncertainty analysis for the calculation of the thermal power

Former literature stressed how critical uncertainty analysis is in the context of HVAC and heat recovery applications [55,56]. However, it was impossible to use measurement technology that recorded the air volume rates (e.g., measurement fans or the Fan Assessment Numeration System, FANS. This resulted in some challenges (see Sections 2.3, 2.4, and 3.6). The calculation of the air flow rates (see sections 2.3 and S3) nevertheless allowed the calculation of the thermal power in the investigated barn building (and subsequently the $COP_{heating}$ and $PF_{heating}$, respectively). However, compared to the measurement techniques mentioned above, this approach has a higher inaccuracy: As Calvet et al. [58] report, this is to be estimated with an inaccuracy of 20%, while measuring fans or FANS only show a value of < 5%.

The subject literature showed that an earlier study [34] used Huggins [57] to calculate the uncertainty. The same procedure was applied here.

The calculation was made according to the following equation [34, 57]:

$$\omega_{\dot{Q}_{HR}} = \left[\left(\frac{\partial \dot{Q}_{HR}}{\partial \dot{m}_2} * \omega_{\dot{m}_2}\right)^2 + \left(\frac{\partial \dot{Q}_{HR}}{\partial (t_{22} - t_{21})} * \omega_{t_{22}-t_{21}}\right)^2\right]^{0.5}$$

where:

$\omega_{\dot{Q}_{HR}}$ = magnitude of the uncertainty of the calculated thermal power for a given measurement period

$\omega_{\dot{m}_2}$ = magnitude of the uncertainty of the calculated supply air mass flow, 20% (of the actual supply air mass flow rate in the corresponding measurement period) given by Calvet et al. [58]

$\omega_{t_{22}-t_{21}}$ = magnitude of the uncertainty of the calculated temperature difference between supply air t_{22} and fresh air t_{21}. The value for each temperature measurement was also used for the temperature difference. It was calculated from the mean accuracy of the four temperature sensors used (for the WTR 190-A1-1A2/PT1000 sensors, the mean of t_{22} and t_{21} in the corresponding interval was applied).

Figure S3 shows the resulting uncertainties. The mean uncertainty $\omega_{\dot{Q}_{HR}}$ was 9.20 ± 3.34 kW or 26.3% ± 32.8%, respectively. The absolute uncertainty [kW] shows a strong linear correlation to the absolute magnitude of the thermal power (see Figure S3.A1 and S3.A2). The deviation from the correlation increases at lower thermal power values. This is not so much due to the uncertainty of the air mass flow rate determination (constant uncertainty of 20%) but to the uncertainty of the temperature sensors or the resulting temperature differences. The increasing uncertainty of the WTR 190-A1-1A2/PT1000 sensors at higher temperatures leads to the fact that small heating powers (resulting from small temperature differences of t_{22} and t_{21}) at high temperatures of t_{22} and t_{21} have stronger absolute uncertainties than small differences at cold temperatures of t_{22} and t_{21}.

For relative uncertainty, the course of the values shows a distinct regressive correlation concerning the absolute magnitude of the thermal power (see Figure S3.R1 and S3.R2). The outliers (0.97% of the values are $\omega_{\dot{Q}_{HR}}$ > 100%; Maximum $\omega_{\dot{Q}_{HR}}$ = 2,553.2%) are here mainly due to the relation between the measurement accuracy of the temperature sensors (relatively constant at 0.438 ± 0.002 °C, see Section 2.2) and the minimal temperature differences (due to

small thermal power and the averaging of several sensor values, the minimum value of the difference is 0.002 K). The limitation of the sensor number or rounding of the temperature averages would limit this problem but would cause other difficulties (e.g., defective or faulty sensors, third type error [58]). With increasing thermal power, the measurement error of the temperature sensors becomes relative, and the inaccuracy $\omega_{\dot{Q}_{HR}}$ asymptomatically approaches a value of about 20%. This corresponds to the assumed inaccuracy of the volume flow calculation.

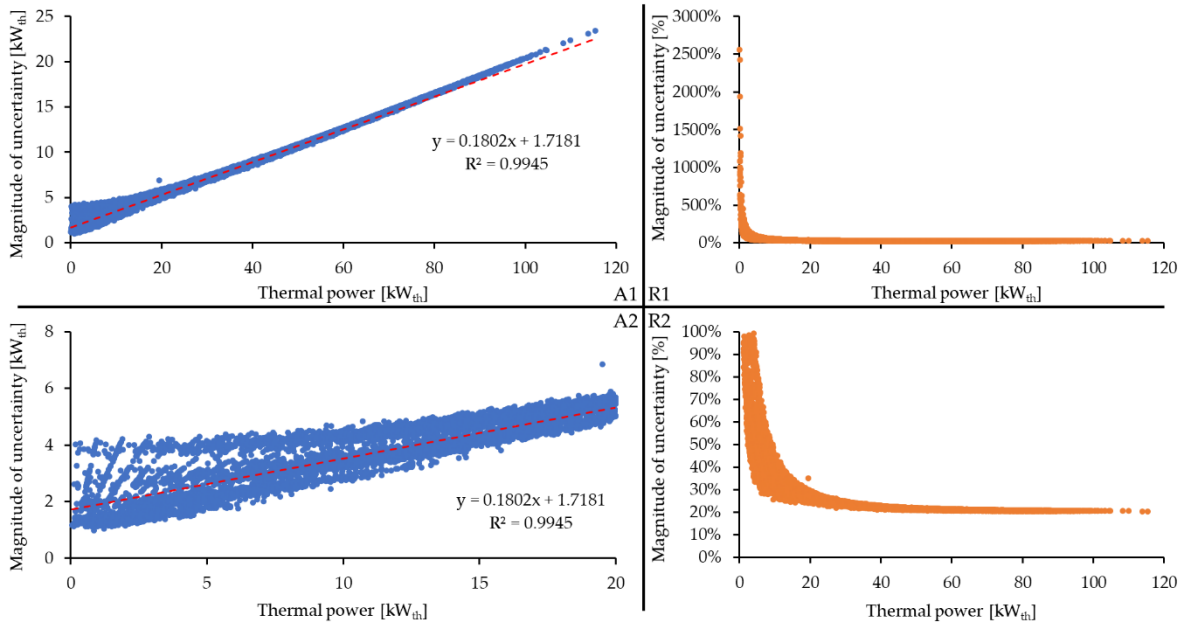

Figure S3. Magnitude of uncertainty $\omega_{\dot{Q}_{HR}}$ on absolute [kW_{th}] or relative [%] base for the calculated thermal power depending on the thermal power [kW_{th}]. A2 shows 7,378 of the 55,435 values (13.30%), and R2 shows 54,894 values (99.02%).

The overall uncertainties were calculated using the aggregated uncertainties of the measurements using the following equation [55]:

$$\omega_{Q_{HR}} = \sum_{i=1}^{55,435} \omega_{\dot{Q}_{HR,i}}$$

where:

$\omega_{Q_{HR}}$ = magnitude of the uncertainty of the calculated thermal power for the complete two-year trial (for the two-year trial, a total of 55,435 measurement intervals were usable)

$\omega_{\dot{Q}_{HR}}$ = magnitude of the uncertainty of the calculated thermal power for a given measurement period

The overall uncertainty of thermal power calculation $\omega_{Q_{HR}}$ was 21.0%.

The same approach was used to calculate the uncertainty of the $COP_{HR,heating}$, respectively. For this purpose, the uncertainty of the thermal power $\omega_{\dot{Q}_{HR}}$ was used, and the uncertainty of the electrical power input of the fans to operate the heat recovery $\dot{Q}_{HR,el}$ (see Sections 2.7, 3.3, and S5). The electrical power input of the exhaust fans was determined by software readout in preliminary field tests (see Section S3). The increasing divergence with higher analog control

could lead to higher uncertainties at high fan speeds of the corresponding exhaust air fans. However, no clear information is available on the accuracy of the output values. For the derivation of the electrical power input of the supply air fans (electricity meter during the different control in pre-tests in the barn building), no accuracies are available either. Consequently, an uncertainty of 20% was also assumed since, in part, the data or software of the manufacturer (exhaust air fans) was used. The authors assume that the real uncertainty is considerably lower, but quantification is impossible.

The mean uncertainty $\omega_{COP_{HR,heating}}$ was 1.93 ± 1.51 or $30.6\% \pm 48.3\%$, respectively. The outliers indicated a maximum of 240.51 or 2,227.6%, respectively. The overall uncertainty of thermal power calculation $\omega_{COP_{HR,heating}}$ was 25.5%.

The discussion of the trials' limitations and uncertainty analysis can be found in Section 3.6.

S5. Calculation of the daily LNG consumption

The LNG consumption was documented via the ordered quantities over the two-year trial period and the gas tank level. The daily consumption was calculated using the period between the deliveries and the delivered quantities. Subsequently, the daily consumption was correlated with the mean of daily mean outside air temperatures for each period. Figure S4 shows this correlation.

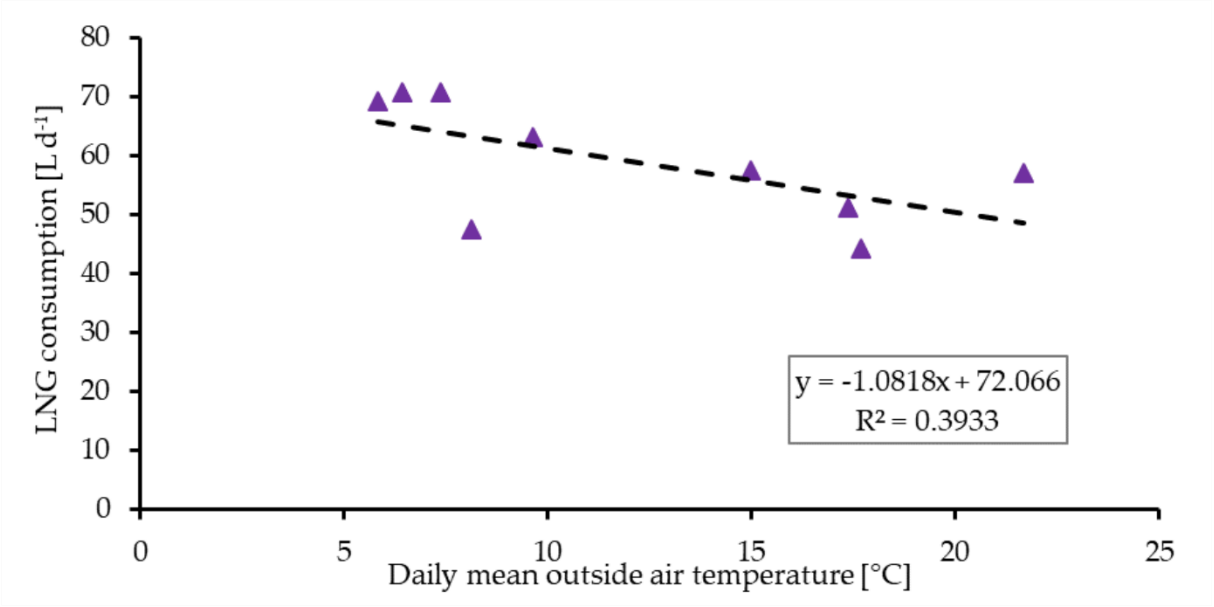

Figure S4. Daily LNG consumption [L d^{-1}] depending on the daily mean outside air temperature [°C].

Based on the correlation shown, the daily LNG consumption was calculated for each trial day. This daily consumption was divided by 96 for all measurement intervals per day (regardless of the outside air temperature in the individual intervals).

The correlation shown can be considered weak ($R^2 = 0.3933$). Nevertheless, there was a minimal deviation between the cumulative LNG quantities calculated this way and the quantities purchased (+2.3%, see section 2.3). Consequently, the approach was considered sufficient.

S6. Calculation of the electrical energy consumption of the exhaust air fans in Case 2

(fan type: A3G990-AZ02-35, ebm-papst Mulfingen GmbH & Co. KG, Mulfingen, Germany)

The calculation took place in several steps for each 15-minute interval in which the supply air fans were operating:

1. The absence of the heat recovery system has several implications for the ventilation system and the operating parameters:
    a. supply air fans are no longer necessary,
    b. supply air is no further conveyed into the barn building; the negative pressure of the exhaust air ventilators conveys the complete air flow in the ventilation,
    c. this increases the amount of negative pressure (negative pressure difference) directly in front of the exhaust fans in the central exhaust air collection duct (see Figure S3).
    d. all exhaust air ventilators convey exhaust air out of the central exhaust air collection duct and not out of the heat exchanger.

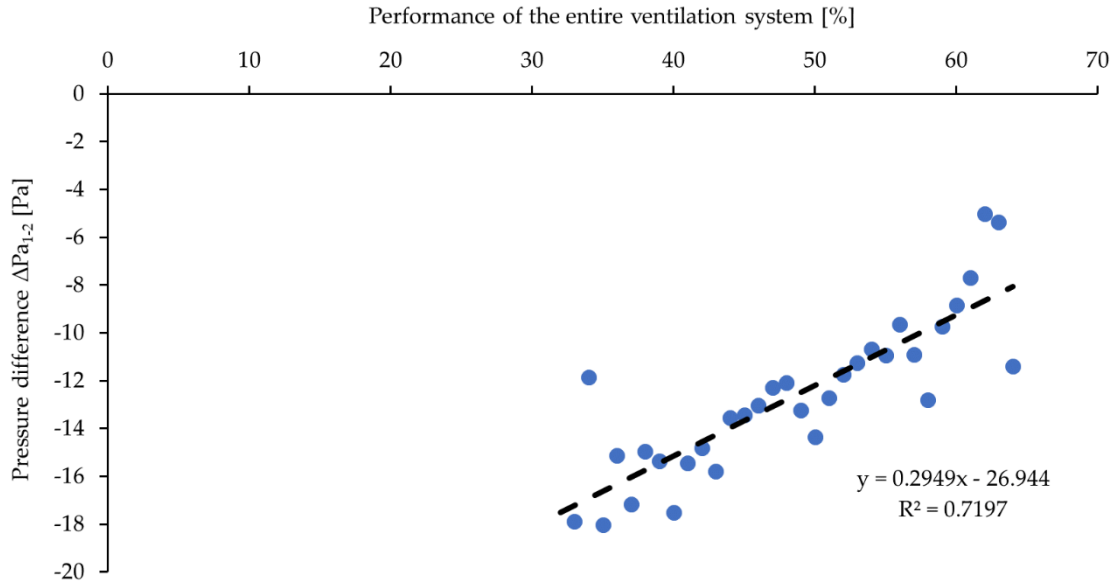

Figure S5. Pressure difference $\Delta Pa_{1\text{-}2}$ [Pa] ($\Delta Pa_{1\text{-}2} = Pa_1 - Pa_2$) within the central exhaust air collection duct due to the absence of supply air ventilators (Pa_2, Case 2, without heat recovery and supply air fans) compared to the actual ventilation system operation (Pa_1, Case 1, with heat recovery and supply air fans) depending on the performance of the entire ventilation system [%]. These pressure differences $\Delta Pa_{1\text{-}2}$ were derived by the data of the 15-minute measurement intervals during the ongoing trial (differential pressure in the central exhaust air collection duct with turned on/off supply air fan; n = 2366 intervals for the mean value calculations of all integer performance values). For example, at 40% performance of the entire ventilation system following differential pressure compared to the atmosphere applied in the central exhaust air collection duct:
36.30 Pa for Pa_1 (Case 1, with heat recovery), -21.04 Pa for Pa_2 (Case 2, without heat recovery),
and the corresponding pressure difference $\Delta Pa_{1\text{-}2}$ of -15.26 Pa ($\Delta Pa_{1\text{-}2} = Pa_1 - Pa_2$).

2. The theoretical differential pressure Pa_2 within the central exhaust air collection duct [Pa] was calculated based on the real differential pressure Pa_1 and the pressure differences $\Delta Pa_{1\text{-}2} = Pa_1 - Pa_2$ shown in Figure S3.

3. The pressure differences [Pa] between the central exhaust air collection duct (Pa_2, Case 2) and the pressure chamber beneath the bio-scrubber were used to calculate the needed fan speeds [n min^{-1}] to convey the given air volume flow rates (the same like the one in Case 1) [m^3 h^{-1}] using the equations explained in Section 2.3 and Section S3.
4. The derived fan speeds [n min^{-1}] were used to calculate the fans' needed analog control [V] to ensure these fan speeds. Subsequently, the analog control [V] was used to calculate the electric power input [W] of the fans in this theoretical operation situation (Case 2).
5. The electric power inputs [W] of Case 1 and 2 were used to calculate the energy consumption $Q_{HR,el}$, the electrical energy consumption to operate a heat recovery system (two heat exchangers) in the barn building's ventilation system.

S7. Results and Discussion – Supplementary Figures & Tables

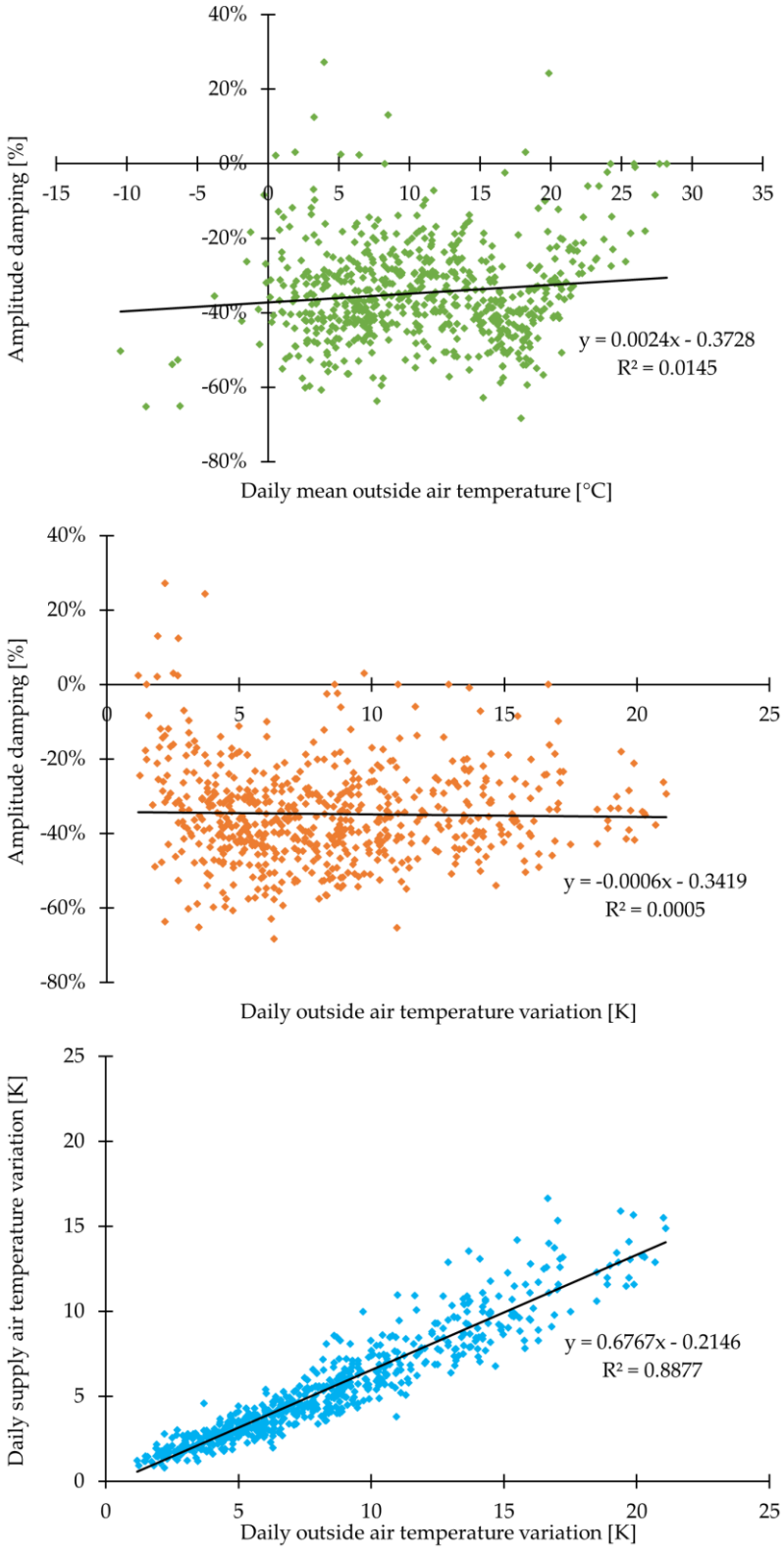

Figure S6. Correlation of amplitude damping [%] and daily supply air temperature variation [K] depending on the daily mean outside air temperature [°C] or daily outside air temperature variation [K]. Temperature variation: Difference between the (daily) minimum and maximum temperature. In the context of the conducted study, amplitude damping refers to the ability of the heat exchangers to reduce the supply air temperature variation Δt_{22} compared to outside air temperature variation Δt_0. The values represent 635 days within the two-year measurement period (see Section 2.8).

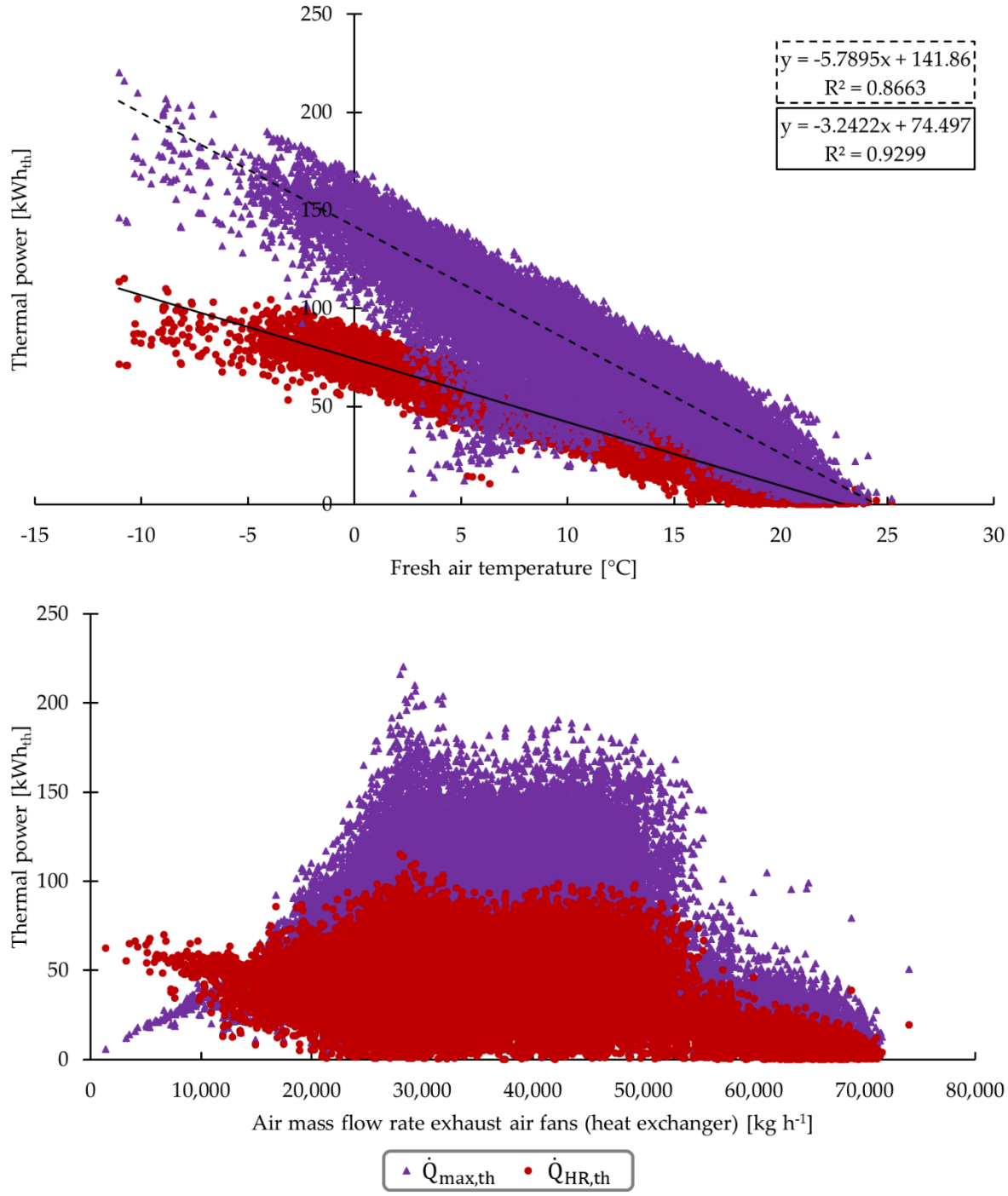

Figure S7. Correlation of the actual thermal power $\dot{Q}_{HR,th}$ and the maximum possible thermal power $\dot{Q}_{max,th}$ [kW_{th}] of the two heat exchangers and the fresh air temperature t_{21} [°C] in the upper diagram, or air mass flow rate of the exhaust air fans (heat exchanger) [kg h^{-1}] in the lower diagram, respectively, when heat exchangers heated the incoming fresh air.

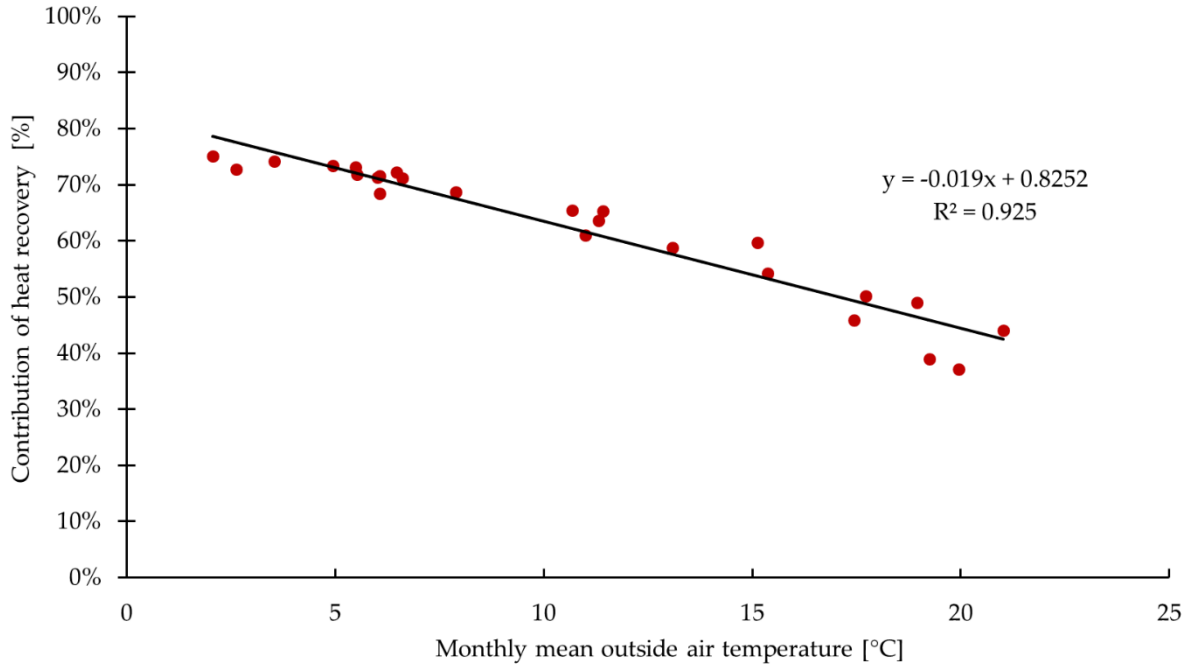

Figure S8. Correlation of the contribution [%] of recovered heat $Q_{HR,th}$ using the heat exchangers from the total thermal energy supply in the barn building $Q_{total,th}$ (heat recovery $Q_{HR,th}$ plus LNG combustion $Q_{LNG,Case1,th}$) and the monthly mean outside air temperature [°C]. Values are based on the monthly cumulated sums over the two-year trial.

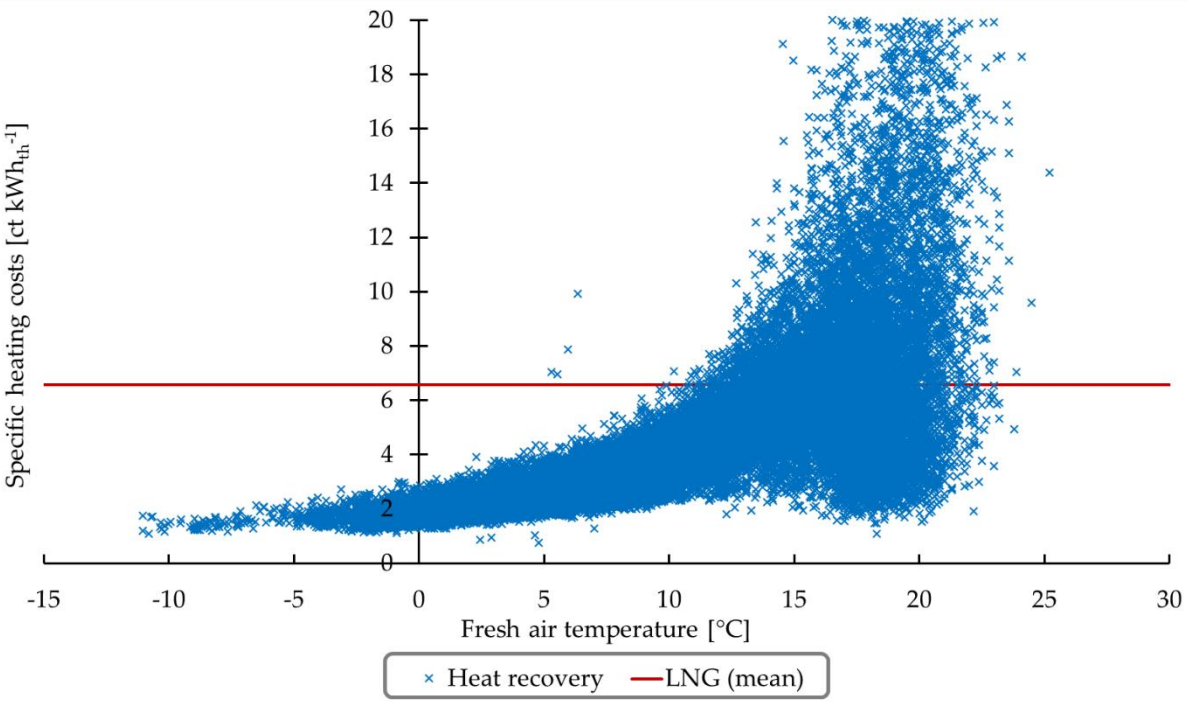

Figure S9. Correlation of the specific heating costs [ct kWh_{th}^{-1}] of the two heat exchangers and the fresh air temperature [°C] when heat exchangers heated the incoming fresh air. The calculated values are based on the substituted LNG costs (6.58 ± 1.69 ct kWh_{th}^{-1}) and the extra electrical energy costs (26.97 ± 0.30 ct kWh_{el}^{-1}) using the heat recovery. This figure shows an excerpt (98.66% of total values); some single outliers show values of up to 3660.92 ct kWh_{th}^{-1}. However, 87.18% of all values are below 6.58 ct kWh_{th}^{-1}, and thus the specific heating costs of heat recovery are lower than the average LNG costs. LNG = liquefied natural gas.

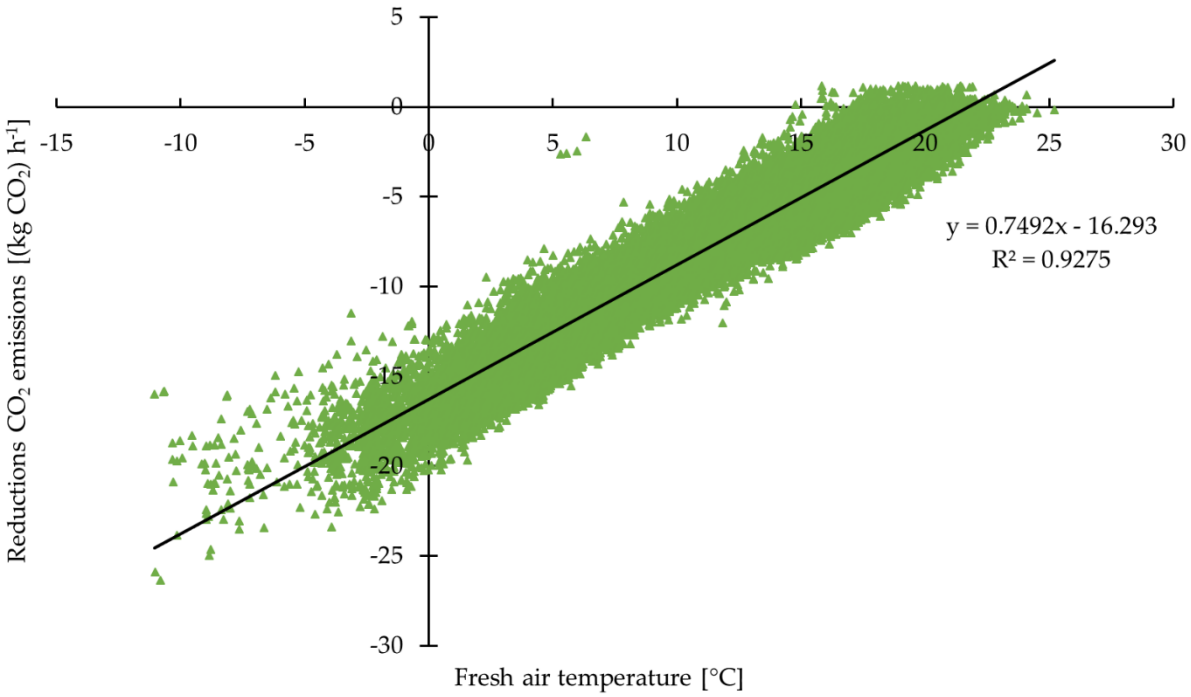

Figure S10. Correlation of the CO_2 emissions reductions [(kg CO_2) h^{-1}] using the two heat exchangers and the fresh air temperature [°C] when heat exchangers heated the incoming fresh air. The calculated values are based on the substituted CO_2 emissions based on LNG combustion [0.237 (kg CO_2) kWh_{th}^{-1}] and the CO_2 emissions based on electrical energy consumption [0.427 (kg CO_2) kWh_{el}^{-1}] using heat recovery.

Table S3. Simplified economic analysis and payback period calculation of the two heat exchangers based on the

	Unit	Case 2: without heat exchanger	Case 1: with heat exchanger
Initial capital cost[A]	EUR	111,600	119,900
… of **which heating system**	EUR	111,600	53,500
… of **which heat recovery system**	EUR		66,400
Annual fixed costs[B] **(depreciation 15 years)**	EUR a^{-1}	7,750	8,500
Annual variable costs[C]	EUR a^{-1}	38,900	33,050
... of which energy cos**ts**	EUR a^{-1}	36,150	30,350
Total annual costs	EUR a^{-1}	46,650	41,500
Payback period			
... of the heat recovery system	a		13.0
... of total investment difference between Case 1 and 2	a		1.6

results in year 1 under the experimental conditions.

A Including the heating system (i.e., the heating system itself and the LNG tank), the heat recovery system, and the assembly costs.

B Including the interest rate (0.5%), the depreciation (15 years), and the insurance.

C Including the energy operating costs (for operating the heating, ventilation and exhaust air purification system), the water costs for cleaning the heat exchangers, the labor costs for cleaning and maintenance the heat exchangers and heating system, and the repair costs (2% of investment) for operating the heat exchangers and the heating system.